Assignment

Homework HL2

Enrico Dalla Mora - 10937966
Michele Murciano - 10883559

Musical Acoustics

POLITECNICO
MILANO 1863

December 4, 2023

Design and Analysis of Spherical Helmholtz Resonators

a) Diameter evaluation

Given the geometry pictured in figure (1), it is needed to compute the diameter D of the sphere characterizing the resonator for a target resonance frequency of 300 Hz. In order to do so the expression relating the fundamental frequency of an Helmholtz resonator with its geometry must be employed:

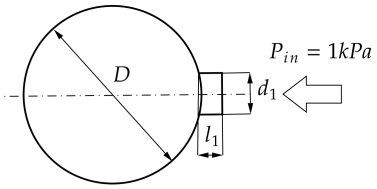

Figure 1: Helmholtz resonator geometry in the first configuration.

$$f_0 = \frac{1}{2\pi}\sqrt{\frac{K}{m}} = \frac{1}{2\pi}\sqrt{\frac{\rho S^2 c^2}{V\rho SL}} = \frac{c}{2\pi}\sqrt{\frac{S}{VL}} \tag{1}$$

Considering the volume of a sphere to be $V = \frac{4}{3}\pi r^3$ the result for the desired diameter D can be obtained as follows:

$$D = \sqrt[3]{\frac{3}{2}\frac{c^2 S}{\pi^3 L f_0^2}} = 0,1406\ m \tag{2}$$

where S is the cross-section of the neck and L represents its acoustic length which is given by:

$$L = l_1 + \Delta = l_1 + \alpha\frac{d_1}{2} \tag{3}$$

The acoustic length correction Δ depends on the structure geometry and it is introduced in order to consider the non ideal case in which the acoustic pressure node is no longer located at the outlet of an open pipe but it occurs slightly further outside the end of the duct. Under low ka condition, the correction factor α can be regarded as constant and equal to 0.6 for unflanged pipes and 0.85 for flanged pipes. Anyway, it's important to notice how the neck of the resonator is neither properly flanged nor unflanged at the connection with the sphere. Therefore the correction factor α for the new acoustic length has been set to 0.93 by an experimental evaluation conducted in the next section. This correction is valid under low ka conditions ($ka < 0.1$), which will correspond to frequencies lower than 272 Hz for $d_1 = 0.04\ m \rightarrow a = 0.02\ m$. Even though, for simplicity purposes, a constant α will be adopted in this study, the virtual elongation model could be extended to values of ka up to 3, according to the graph in figure (2).

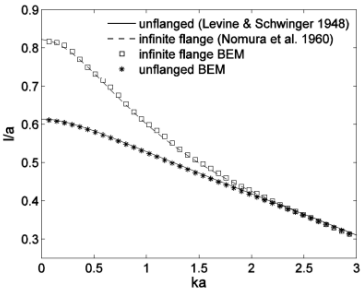

Figure 2: Correction factor α as a function of ka.

Comsol model implementation

In order to evaluate the input impedance of the above mentioned resonator let's first discuss the implementation of the model in Comsol.

- Geometry

The system can be modelled by employing a 2D axisymmetric geometry. This approach will be much more efficient then building the same model in 3D, both in mesh building and studies computation. Values for d_1 and l_1 have been added as parameters in order to compute the parametrical sweeps needed in the next sections. On the other hand, the diameter D will remain constant regardless of the value of d_1. The height of the rectangle constituting the neck of the resonator has been set in order to have $\overline{AB} = l_1$ (figure 3). Therefore the actual rectangle height is arbitrarily bigger than l_1 as for the geometry to be consistent. Finally, the union between the domains automatically eliminates the interior boundaries.

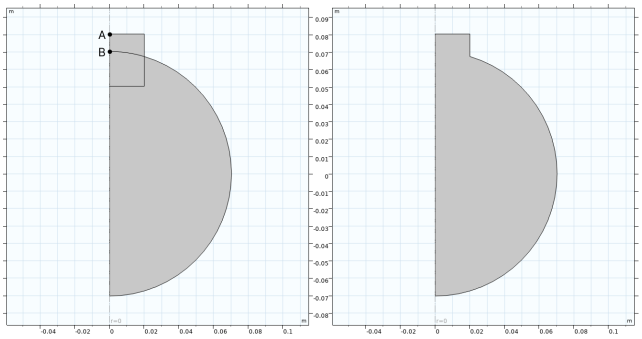

Figure 3: Geometry components and merged configuration in Comsol.

- Mesh

The mesh needs to be properly defined in order to avoid spacial aliasing. In particular, the maximum element size must respect this condition:

$$l_{max} < \frac{\lambda}{10} = \frac{c}{10\, f_{max}} \tag{4}$$

In the case under analysis, being the maximum frequency of study $f_{max} = 10000\ Hz$, the element size for the mesh needs to be smaller than $3,43\ mm$.
This condition is satisfied by the maximum element size automatically computed by the Comsol configuration once it has been calibrated for *fluid dynamics* (in particular, the resulting maximum element size is equal to $3,16\ mm$). Furthermore, in order to achieve a better accuracy of the viscous behaviour near the boundaries of the domain, the size of the mesh elements has been reduced close to the edges.

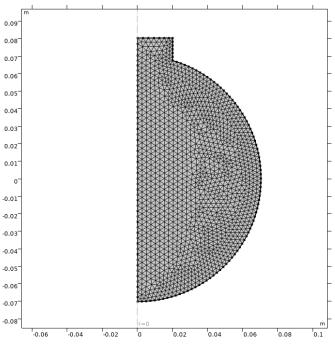

Figure 4: Comsol model mesh.

- Physics

The length scale at which the thermoviscous acoustic description is necessary, depends on the thickness of the viscous boundary layer which is given by the following formula:

$$\delta_v = \sqrt{\frac{\mu}{\pi f \rho}} \tag{5}$$

where μ is the dynamic viscosity of the fluid and ρ is its density. In the case under analysis, the lowest frequency is 10 Hz and the considered fluid is air, therefore the maximum thickness of the boundary layer will result as $0,71$ mm which is clearly negligible with respect to the smallest dimension of the geometry which is 1 cm, the diameter of the smallest neck considered. For this reason, not only it's unnecessary to employ the thermoviscous physics, but also the viscous boundary layers for the pressure acoustics physics can be neglected. This being said, the pressure acoustics physics has been adopted and the fluid model has been set to viscous. Finally, a pressure of 1000 Pa is applied to the inlet of the resonator.

- Probes

Before computing the studies, probes for pressure ($acpr.p\_t$) and velocity ($acpr.v\_tz$) of the fluid at the neck entrance have been created in order to later compute the input impedance of the resonator.

b) Input impedance for $d_1 = 4$ cm

The acoustic impedance at a given surface is defined as the ratio between the acoustic pressure over the surface $P(\omega)$ and the acoustic volume flow through it $U(\omega)$:

$$Z(\omega) = \frac{P(\omega)}{U(\omega)} \tag{6}$$

Let's then compute a frequency domain study in the range $10 - 10000$ Hz with a 10 Hz step. The probes table for pressure and velocity calculated by the study are then exported into Matlab in order to achieve a proper graphical representation of the impedance. The resulting graph is reported below. As expected, the first minima of the impedance, which represents the fundamental resonance of the resonator is tuned at 300 Hz. This result is achieved by an experimental evaluation of α, the correction factor for the acoustic length of the input pipe. As can be seen form the above image, the zero pressure node, which corresponds to the white line, does not coincide precisely with the end of the neck. The exceeding length is in fact taken into account by the correction factor.

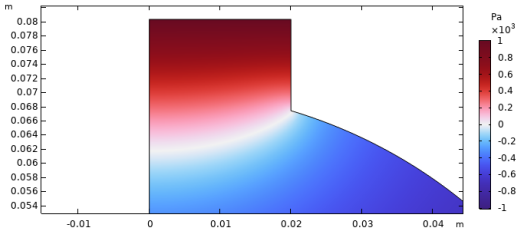

Figure 5: Pressure distribution in the neck at 440 Hz.

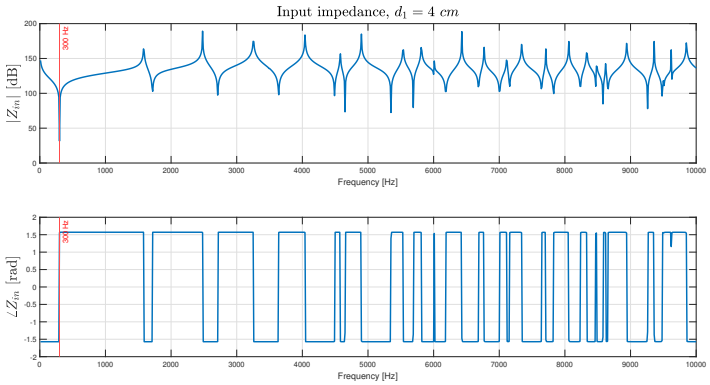

Figure 6: Input impedance for neck diameter $d_1 = 4$ cm.

As can be seen from the graph, resonances higher than the fundamental one manifest as a consequence of the interaction between the pipe and the cavity.

c) Input impedance for $d_1 = 1, 3, 8$ cm

It is now needed to compute the same study for varying values of d_1 but keeping the diameter of the sphere D calculated in section (1) fixed. The reported results in figures 7-8-9 show how resonance frequencies are strictly dependent upon the diameter of the neck. In particular, for increasing values of the diameter d_1, the resonance frequencies will be shifted upwards. This phenomenon is more evident looking at the first resonance frequency which is highlighted in the graphs. It's important to notice anyway that the previous discussion on the thermoviscous physics and mesh max element size will still be valid.

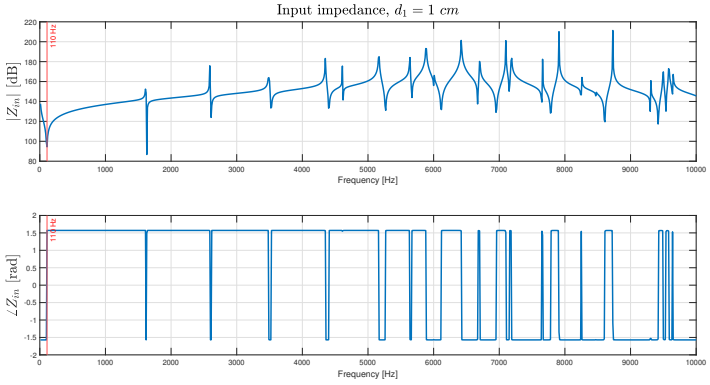

Figure 7: Input impedance for neck diameter $d_1 = 1$ cm.

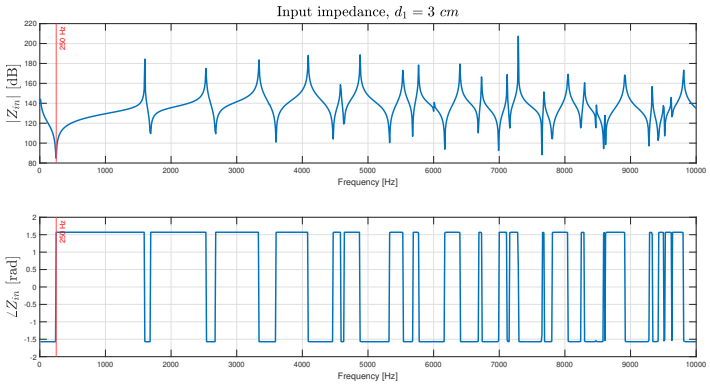

Figure 8: Input impedance for neck diameter $d_1 = 3\ cm$.

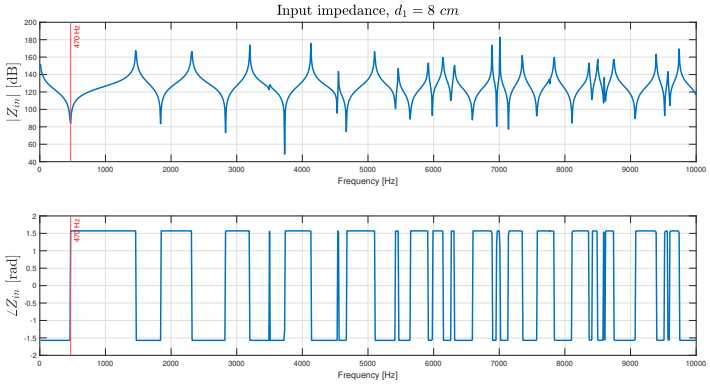

Figure 9: Input impedance for neck diameter $d_1 = 8\ cm$.

d) Modal analysis

Let's now evaluate the different contributions of various excitation modes (figure 10) for the various diameters d_1. In order to do so, a modal sweep must be employed with sweeping parameters d_1 and the azimuthal mode number m. The results for the various cases are reported in figure (figure 11). As can be seen from the graphs, the influence of higher modal components on the overall summation is smaller for smaller diameters. If the contribution of higher modes would cancel resonances and antiresonances of lower modes, a much smoother input response would be obtained. However, this is not the case and therefore the best resonator, with less resonances apart for the first one, will result to be the one with the smallest diameter $d_1 = 1\ cm$.

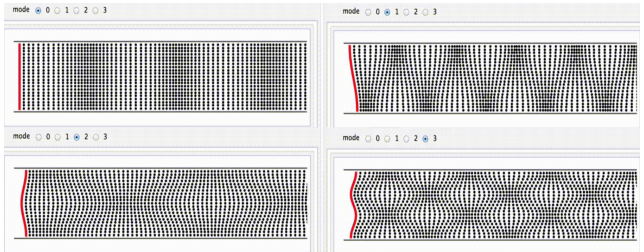

Figure 10: Excitation modes varying the azimuthal mode number.

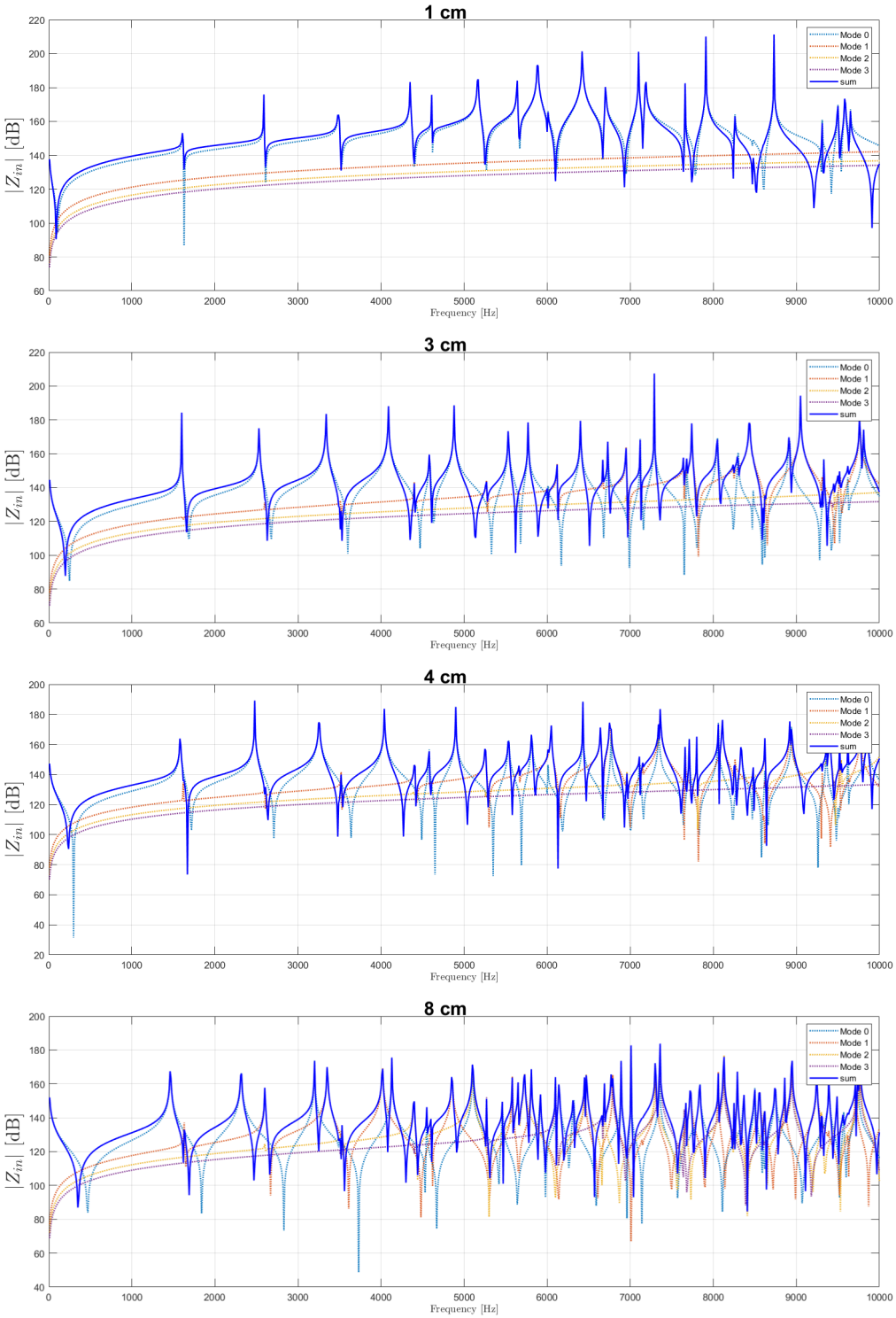

Figure 11: Input impedance for the first four modal components and their sum for varying d_1.

As can clearly be seen from the above figures, modes present a cutoff frequency below which there is a reduction of about 10 dB within a distance smaller than the radius of that

tube. This means that below that frequency, there are no resonances and antiresonances. The cutoff frequency ω_c for a specific mode q_{mn} and diameter d_1 is described by the following relation:

$$\omega_c = \frac{\pi q_{mn} c}{a} \tag{7}$$

Note that, for the mode $(0,\ 0)$ there is no cutoff frequency since $q_{mn} = 0$ and therefore resonances will manifest in the low frequency range. It is also important to notice that the cutoff frequency is inversely dependent on d_1 and consequently for bigger diameters resonance frequencies of higher modes appear at lower frequencies, affecting the overall summation.

e) Double resonator simulation in Comsol

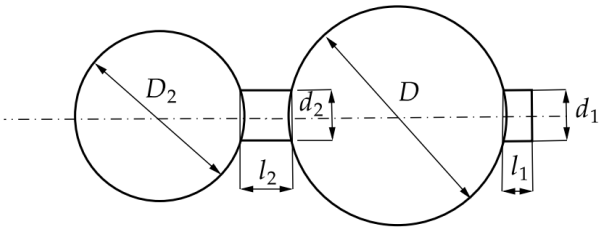

Figure 12: Double resonator geometry configuration.

The model for the coupled configuration presented in figure (12) is obtained following the same procedure as in section 1. Note that the discussions previously made on the maximum element size for the mesh, the thickness of the viscous boundary layer and on the virtual elongation of the pipe are still valid. In particular, the neck's diameter of the first resonator d_1 has been set to $0.01\ m$ in order to consider the best resonator configuration. The results of the simulation are shown below:

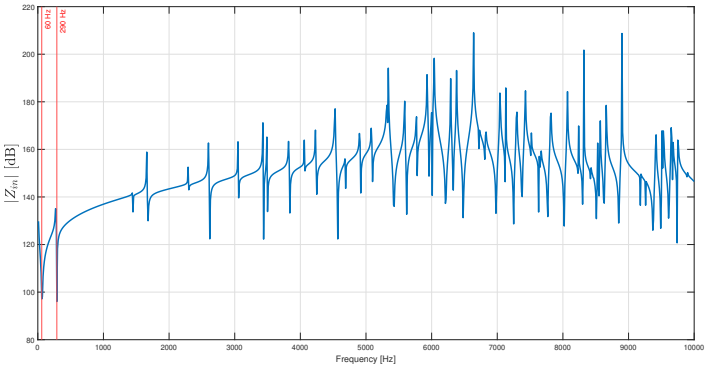

Figure 13: Input impedance for the coupled resonators.

As can be seen in the above figure, the coupled resonator has two main resonances in the low frequency range. As expected, these two resonances arise as a consequence of the coupling between the two resonators. The coupling will also manifest in the higher frequency region with many different resonances with respect to the case of the single resonator.

f) Electric analogue

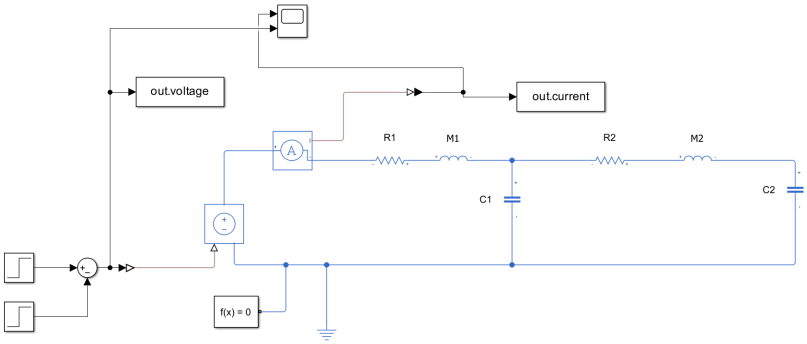

Figure 14: Equivalent circuit of the double resonator.

In order to simplify the analysis of the double resonator configuration it is possible to describe its acoustic network via an analogous electric one. In particular, the equivalent circuit shown in the figure above has been obtained adopting the *impedance analogy* according to which an equivalence can be established between pressure p and voltage v (potential-type quantities), acoustic volume flow U and current i (flux-type quantities).
Each resonator is composed by two fundamental acoustic elements: the neck of the resonator constitutes a pipe and the air that is moving through it possesses a finite mass, thus the neck represent the inertial component (acoustic mass M_a) of the system; the oscillation of the air column inside the neck contributes to the expansion and compression of the air in the closed volume, causing the pressure in the spherical cavity of the resonator to increase and decrease; thus, the air in the cavity can be thought as an "acoustic spring" characterized by an acoustic compliance C_a. A full equivalent circuit description of the resonator has been obtained including also the acoustic radiation resistance R_a caused by the dissipated energy at the interface between the pipe and the cavity when the fluid moves through it.
Once the acoustic elements have been identified, it is possible to define their equivalent electrical elements according to the following table based on the analogy introduced before:

Impedance analogy ($p \leftrightarrow v, U \leftrightarrow i$)			
Acoustic domain		Electric domain	
Acoustic element	Acoustic law	Equivalent electric element	Electric law
Acoustic mass $M_a = \frac{\rho l}{S}$	$p = j\omega M_a U$	Inductor with $L = M_a$	$v = j\omega L i$
Acoustic compliance $C_a = \frac{V}{\rho c^2}$	$p = \frac{1}{j\omega C_a} U$	Capacitor with $C = C_a$	$v = \frac{1}{j\omega C} i$
Acoustic resistance R_a	$p = R_a U$	Resistor with $R = R_a$	$v = Ri$

Finally, to create the equivalent circuit model of the double resonator, the following connection rules have been employed: different elements sharing the potential-type variable p have been connected in parallel in the equivalent circuit; conversely, different elements sharing the flow-type variable U have been connected in series.
It is extremely important to notice that the use of this electro-acoustic analogy allows for the characterization of acoustical systems using networks of *lumped* electrical elements. This procedure obviously has a limit of validity and application in the acoustical domain in which the discretization of spatially distributed elements into lumped ones gives reliable results only when the signal wavelength λ is much greater than the largest dimension L of the device under consideration, i.e. $\lambda >> L \ \rightarrow \ \lambda > 10L$.
In this case the resulting frequency below which the lumped element assumption is satisfied is around 217 Hz. It will anyway be considered to be acceptable up to the resonance frequency of around 290 Hz.

With the new geometry, another correction factor must be introduced in order to take into account for the virtual elongation of the second pipe, the one connecting the two resonators. This time the pipe is connected on both sided, therefore the correction factor is expected to be more or less double the one obtained for the single-connected pipe. This being said, an experimental evaluation has led to a value of $\alpha_2 = 1.8$ which is perfectly coherent with the beforementioned considerations. This value will represent a good approximation in the calculation of the electrical parameters which will then result in a input impedance very similar to the one obtained in Comsol, at least for low frequencies (see figure 16).

The input voltage signal has been set to an impulse obtained by subtracting two steps distant $\frac{1}{Fs}$ seconds from one another. Fs is the chosen sampling frequency which, according to Nyquist theorem, has been set to double the maximum frequency to be analyzed (10000 Hz). This will allow to avoid aliasing when computing the Fourier transform of the signals. Furthermore, the resistances R_1 and R_2 are being set to an arbitrary value of 500 Ω which will allow for a better representation of resonances and for a much clearer comparison with the Comsol results. This choice will only affect the magnitude of the calculated input impedance, thus will not affect the physical accuracy of the model.

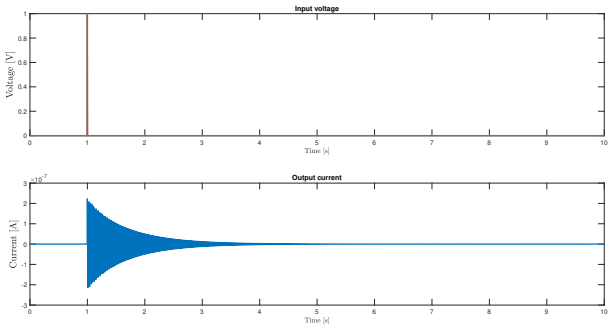

Figure 15: Time domain signals for voltage and current.

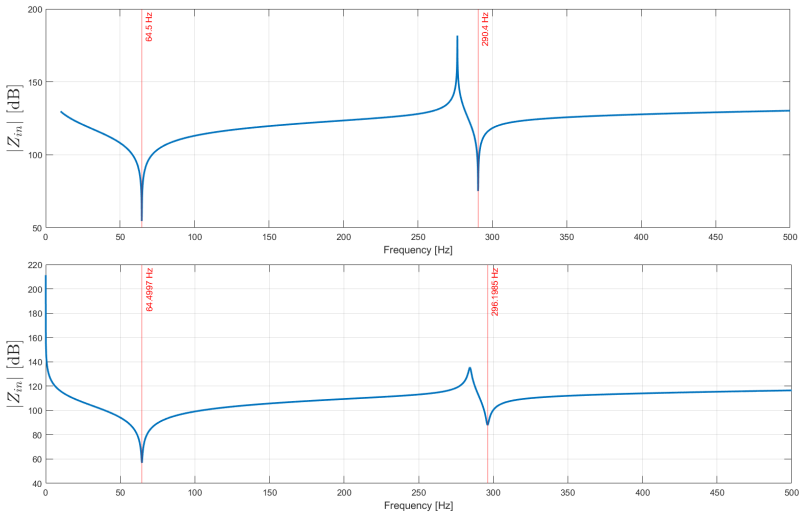

Figure 16: Input impedance obtained from Comsol (top) and Simulink (bottom).

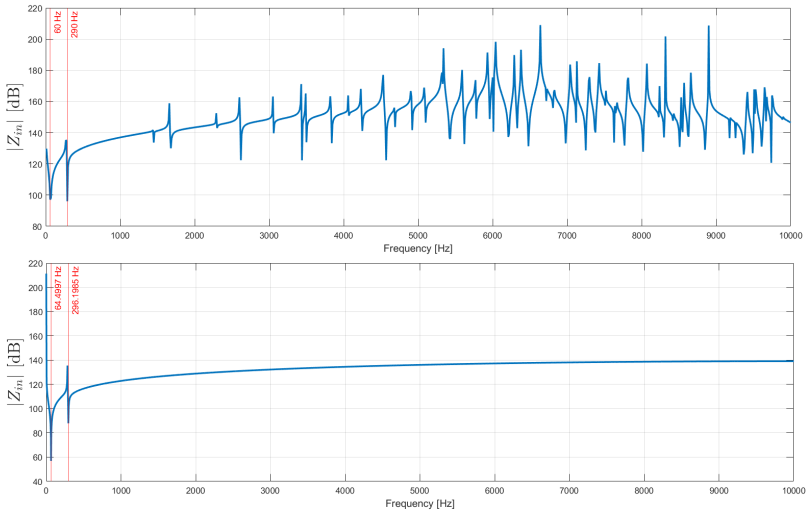

Figure 17: Input impedance obtained from Comsol (top) and Simulink (bottom) up to 10 kHz.

As can be seen from the above figures, the electrical model approximates very well the input impedance obtained in Comsol but only at low frequencies. This is due to the lumped element condition discussed before. All higher-frequency resonances are in fact missing in the Simulink simulation results since the circuit is made of only two RLC rings. Finally, the graphs also show how the correction factors α_1 and α_2 has been chosen properly.